Journal of the Optical Society of America B
OPTICAL PHYSICS

Path to ultralarge nonlinear-optical susceptibilities

MARK G. KUZYK

Department of Physics and Astronomy, Washington State University, Pullman, Washington 99164-2814, USA (mgk.wsu@gmail.com)

Received 19 August 2016; revised 5 October 2016; accepted 7 October 2016; posted 11 October 2016 (Doc. ID 274111); published 7 November 2016

The search for new materials with ever-larger nonlinear-optical susceptibility is fueled by the promise of new applications. While much progress has been made, no new paradigms have been discovered that lead to significantly larger nonlinear susceptibilities when size has been taken into account. The next breakthrough requires a step back to consider the fundamental requirements for increasing the strength of light–matter interactions. In essence, the problem at hand is to understand how to get the most out of a system of fixed size (defined as the spread in the electronic wave function) that contains a given number of electrons. The intrinsic nonlinearity takes into account size so that the origin of what makes a large nonlinear response can be identified. Only then can a recipe be articulated for making the system larger in a way that scales optimally so that ultralarge nonlinear susceptibilities can become a reality.

OCIS codes: (190.0190) Nonlinear optics; (190.4400) Nonlinear optics, materials.

http://dx.doi.org/10.1364/JOSAB.33.00E150

1. INTRODUCTION

Matter is essentially a localized collection of bound electrons. Optimizing the nonlinear-optical response of a quantum system comes down to using a fixed number of electrons as efficiently as permitted by the laws of physics. The most effective way to use electrons often depends on the size of the system. As such, making the ultimate nonlinear-optical material requires an understanding of how the nonlinear response scales with a quantum system's size. Finally, one must determine how to assemble the units together to make a bulk material.

A large nonlinear-optical response is certainly a common requirement of many devices. However, perhaps the most serious impediment to the development of exceptional new materials is the focus on the magnitude of the nonlinear-optical response without taking into account the size of the system. This approach masks the fundamental properties responsible, thus hampering the development of an understanding of what makes a material's nonlinear susceptibility ultralarge.

Some authors have attempted to take the size into account by normalizing the nonlinear response to the number of electrons or the size of the molecule from its chemical structure [1]. However, these metrics alone are not representative of the true size of the system. A more rigorous approach is to define a quantum size in terms of a system's wave function and number of electrons. This size can then be applied to develop a guide for how the nonlinear susceptibilities should scale for ideal materials. One approach to removing size effects is by defining an intrinsic nonlinearity, which provides an absolute metric of the nonlinear-optical efficiency. This makes possible a direct comparison between quantum systems of differing sizes, thus allowing the important factors leading to a large nonlinear-optical response to be isolated and identified. We will refer to the basic quantum unit as a "molecule," though it could be a metal particle or a complex nanostructure.

The best molecules have intrinsic nonlinear susceptibilities—defined as the nonlinearity normalized to the nonlinearity of an ideal molecule of the same size—that remain large when their size is increased by adding atoms. If the intrinsic nonlinearity is constant with molecular size (recall that the nonlinearity of each molecule is normalized to the nonlinearity of the ideal molecule of the same size), the absolute nonlinearity will grow as a power law of the size, making it possible to attain ultralarge absolute nonlinearities with modest size increase. For example, we will see that the third-order susceptibility scales as L^7, where L is the molecular length. Thus, a molecule whose intrinsic second hyperpolarizability γ is size independent will have an absolute second hyperpolarizability that is 10^7 times larger than a molecule of one tenth the length. The highest-order power laws observed to date in molecules fall well below this rate [2–4], so there is lots of room for improvement.

A comparison of intrinsic nonlinearities of a set of molecules that are related to each other through small changes in a structural feature, such as the placement of a molecular group along a chain or by adding unit cells to a chain, can be used to identify the critical properties for attaining a large nonlinear-optical response [5].

Once the basic quantum units of large nonlinearity are found, they need to be built into a material. Properties that can be varied at the microscopic and macroscopic scales include geometry, topology, potential energy profile, and composition. This brings up the concept of hierarchies, where the requirements of the microscopic units may differ from the assembled system.

The transition from quantum to classical behavior when a system is made larger has not been studied in the context of optimizing the nonlinear-optical response. It has been reported that at room temperature, silver spheres undergo a transition characterized by bulk states, as predicted by quantum mechanics, and surface states that are characteristic of surface plasmons, as described by classical electrodynamics [6]. Because the *largest possible* nonlinear response that originates in quantum excitations is much larger than the *largest possible* nonlinearity originating in a classical phenomena, the ideal system is one that is made of microscopic units whose sizes fall just below the classical threshold, and the units are arranged in a way that optimizes the bulk response. A potentially fruitful approach that has been mostly neglected by the nonlinear-optics community is a search for methods to prevent classical behavior by isolating molecules from the environment or working at low temperature.

Nonlinearity is not always the most important property. Applications demand that several material parameters be optimized together. For example, electro-optic devices require large second-order susceptibility, low loss, and low dielectric constant. To take into account multiple factors, a figure of merit (FOM) can be defined. Since all phenomena ultimately originate in the quantum world, the quantities on which the FOM depend are not independent but are functions of quantum parameters that are calculated from wave functions and energy spectra.

This paper outlines a path to make materials with ultralarge nonlinear susceptibilities, starting with a discussion of the meaning of length, how it applies to molecules, and how it leads to scaling laws of the nonlinear-optical response. These scaling laws are shown to be taken into account by defining intrinsic properties. Classical and quantum systems are rigorously analyzed to show that quantum mechanics provides the winning recipe, and the scaling of 1D and 3D systems is considered to show that a one-dimensional system is ideal. Using the electric dipole approximation, the optimal configuration of a bulk material is proposed based on scaling arguments provided from limit theory. The same can be done in the magnetic dipole approximation, which can be generalized to higher-order electric and magnetic moments.

2. DISCUSSION

This section defines size and scaling and shows how it applies to the nonlinear-optical response.

A. Size and Scaling

The concept of size is a classical one. Here we develop a rigorous quantum definition that enables us to apply it to how the nonlinear-optical susceptibilities depend on size and how size can be taken into account.

A naive definition of the length is the distance between the boundaries beyond which no electron density is found. Using this definition, the stick figures used by chemists to represent molecules can be used to determine this length.

Since the electron density never drops to zero, a better definition is the root mean square deviation

$$L^2 \sim \Delta x^2 = \langle x^2 \rangle - \langle x \rangle^2 = \sum_{n \neq 0} x_{0n} x_{n0}, \tag{1}$$

where x is the aggregate position operator defined by

$$x = \sum_{k}^{N_{el}} x^k, \tag{2}$$

N_{el} is the number of electrons, x^k is the position of electron k, x_{n0} is the $(n, 0)$ matrix element of x, and the expectation values are of the operators in the ground state. Note that Eq. (2) is proportional to the total dipole moment.

Equation (1) gives the square of the length in terms of the electron density, which contains a position operator that is derived from the sum over all of the electrons according to Eq. (1). This length will not necessarily be the same as the size of the stick figure if the charge density accumulates in a small part of the molecule.

Deciding which electrons to count is not a simple task [7,8]. Some of the electrons in a molecule are near the nuclei so are immobile while others serve the purpose of holding the molecule together. A small fraction of the electrons move when excited by light. When studying light–matter interactions, the electrons of interest are the ones that interact with light. In organic molecules, these are often the π electrons. A large response requires that the molecule have many such mobile electrons.

We can determine the upper bounds of the length using the sum rules [9–11]

$$\sum_{n=1}^{\infty} \langle 0|x|n\rangle \langle n|x|0\rangle E_{n0} = \frac{\hbar^2 N_{el}}{2m}, \tag{3}$$

where N_{el} is the number of electrons, m is the electron mass, and $E_{n0} = E_n - E_0$ is the energy difference between states n and 0. Through simple manipulation, the sum rules yield

$$\sum_{n=1}^{\infty} x_{0n} x_{n0} E_{n0} \geq \sum_{n=1}^{\infty} x_{0n} x_{n0} E_{10} = E_{10} L^2. \tag{4}$$

Equations (3) and (4) can be used to get the upper limit of the length, which is given by

$$L_{\max}^2 = \hbar^2 N_{el} / 2 m E_{10}. \tag{5}$$

Thus, there are three lengths: the length of the stick model of the molecule, the quantum length defined by Eq. (1), and the length limit given by Eq. (5). In order to gain an appreciation for the quantum definition of length, we need to first determine how the sum rules are affected by a rescaling of the length by a factor ξ. The position operator must scale in the same way, so we make the transformation $x \to \xi x$. The sum rules, given by Eq. (3), remain invariant only when the Hamiltonian, and thus the energies, are rescaled according to $E \to E/\xi^2$. This makes sense since a larger molecule typically has a lower energy. One can trivially verify this for a particle-in-a-box model of an electron.

As we see in Eq. (5), the length also depends on the number of electrons. Thus, we define the simple scaling transformation to be of the form

$$\text{Simple Scaling Transformation}: \begin{cases} x_{pn} \to \xi x_{pn}, \\ N_{el} \to \eta N_{el}, \\ E_{pn} \to \frac{\eta}{\xi^2} E_{pn}, \end{cases} \tag{6}$$

which leaves the sum rules unchanged. Note that the simple scaling transformation, when applied to Eq. (5), yields $L_{\max} \to \xi L_{\max}$. Thus, simple scaling is the operation of making a quantum system larger.

We are now equipped to understand how simple scaling, the act of making the molecule larger while preserving the sum rules, affects the nonlinear-optical response. Recall that the zero-frequency polarizability α is given by the sum-over-states expression

$$\alpha = 2e^2 \sum_p \frac{|x_{0p}|^2}{E_{p0}}. \tag{7}$$

To determine the upper bound of α, we express it as

$$\alpha = 2e^2 \sum_p \frac{E_{po}|x_{0p}|^2}{E_{p0}^2} \le \frac{2e^2}{E_{10}^2} \sum_p E_{p0}|x_{0p}|^2. \tag{8}$$

Since the term on the right-hand side is just the sum rule, we get the upper bound with the help of Eq. (3), or

$$\alpha_{\max} = \frac{e^2\hbar^2}{m} \cdot \frac{N_{el}}{E_{10}^2} = 2e^2 \frac{|x_{\max}|^2}{E_{10}}, \tag{9}$$

where we have expressed the limit in two different ways. Note that $x_{\max}$ is the largest possible transition moment to the first excited state, which is also the quantum length given by Eq. (1).

Upon simple scaling, the polarizability scales as

$$\alpha \to \frac{\xi^4}{\eta} \cdot \alpha. \tag{10}$$

If we imagine adding unit cells to build a molecule, the length will grow with the number of electrons added, or $\eta \propto \xi$. As such, the polarizability will scale as the volume of the molecule. This is not surprising given that the polarizability has units of volume.

To remove the affects of simple scaling, it is convenient to divide the polarizability of a molecule by the limit to determine its *intrinsic* polarizability, or

$$\alpha_{\text{int}} = \frac{\alpha}{\alpha_{\max}}. \tag{11}$$

The intrinsic polarizability is less than unity and is invariant to simple scaling, so it is an absolute measure of the polarizability; the closer to unity, the better the molecule. As such, the intrinsic polarizability is a convenient way of comparing different molecules, regardless of size. Thus, if one were interested in optimizing the polarizability, one would find a molecule with an intrinsic polarizability near unity. If the molecule is made larger in a way that leaves the intrinsic polarizability constant, the absolute polarizability would increase in proportion to the size.

The same arguments can be applied to the nonlinear susceptibilities. To design the best molecule, one would search first for candidates with the largest intrinsic values. Then, one would make larger versions of the same molecule by adding unit cells. The target would be systems whose intrinsic nonlinearities remain constant with size because the resulting nonlinearity would grow as a power law, making huge nonlinearity possible.

B. Classical versus Quantum Nonlinearity

The previous section implies that arbitrarily large nonlinearity can be obtained by making an ever-larger molecule. However, quantum systems transition to classical ones when made large enough. This can arise when the energy spacing gets smaller than thermal energies or other effects interfere with the coherence of the wave function.

Scholl and coworkers have used transmission electron microscope (TEM) imaging and monochromatic scanning TEM electron energy-loss spectroscopy to probe the transition between quantum and classical behavior. Scholl's group characterizes approximately spherical silver nanoparticles as a function of diameter from 20 nm down to 2 nm [6]. They find a substantial deviation from classical predictions in this range, with a smooth transition between the two, suggesting that this size range defines the quantum/classical interface for the system studied.

Classical behavior is associated with loss of coherence, which washes out interference. Since constructive interference yields nonlinearities near the limit, classical systems will never be as good as quantum ones in terms of most effectively using electrons. Thus, a potentially fruitful research direction would focus on understanding why systems transition to classical behavior with the goal of making larger quantum systems. If interactions with surrounding material is responsible, then isolating a molecule and keeping it at low temperature might be a viable approach.

How classical effects reduce the nonlinearity can be illustrated by comparing a quantum system with a plasmonic one. We start by considering the polarizability in one dimension in the classical and quantum cases.

Figure 1(a) shows a schematic diagram of a slab of material of thickness d, where the largest two faces each have an area A. The thickness is much smaller than any other dimension in the slab, so a uniform applied electric field yields a uniform electric field inside. With dielectric constant ε (sometimes called the

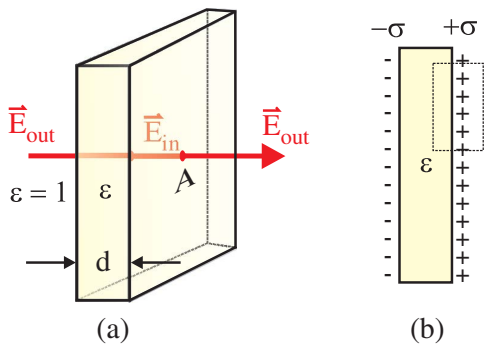

Fig. 1. (a) An electric field applied perpendicular to a slab of thickness d and area A. (b) The induced surface charge density, $\pm\sigma$, forms a dipole moment. Note that throughout this paper, the electric field will be along the dimension labeled d, independent of the area A, even when $\sqrt{A} < d$.

relative permittivity), the electric field inside the slab can be calculated from continuity of the normal component of the electric displacement, yielding $\varepsilon E_{\text{in}} = E_{\text{out}}$. Figure 1(b) shows the induced surface charge, which is given by

$$\sigma = \frac{1}{4\pi}(E_{\text{out}} - E_{\text{in}}) = \left(\frac{\varepsilon - 1}{4\pi\varepsilon}\right)E_{\text{out}}, \tag{12}$$

where $E = E_{\text{out}}$ is the incident field. Equation (12) gives the induced dipole moment of magnitude $p = qd = (\sigma A)d$, or

$$p = Ad\left(\frac{\varepsilon - 1}{4\pi\varepsilon}\right)E. \tag{13}$$

If the slab is much smaller than the wavelength of the incident light, the static field approximation used here holds for time-harmonic fields. As such, the polarizability is then given by $\alpha(-\omega;\omega) = p(\omega)/E(\omega)$, or

$$\alpha(-\omega;\omega) = Ad\left(\frac{\varepsilon(\omega) - 1}{4\pi\varepsilon(\omega)}\right), \tag{14}$$

so it scales as the thickness of the slab. $\varepsilon(\omega)$ is usually calculated with the classical Drude model.

To treat the quantum case, consider a particle in a one-dimensional box of width d, as shown in Fig. 2. From this point forward, the applied electric field will be along the dimension labeled d. With two electrons per state, the N-particle ground state has all single-particle states occupied from $n = 1$ to $n = N_{el}/2$. Then, the lowest excitation energy E_{10} is the energy difference between the highest occupied single-electron state and the lowest unoccupied state energy, so it is given by

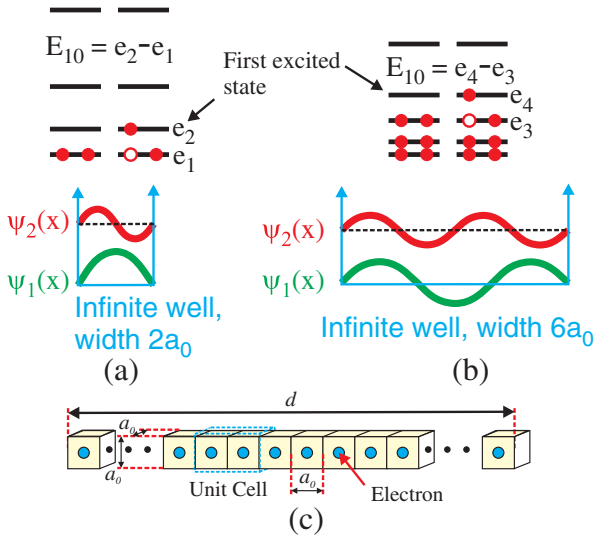

Fig. 2. (a) Two electrons in a box of width $2a_0$. (b) When material is added to the box along d, which is along the applied electric field, the number of electrons grows with the width and the energy-level spacing decreases. The energy eigenfunctions are plotted for the single-particle state at the Fermi energy and the single-particle state just above the Fermi energy. Note that the state energies associated with the transverse quantum numbers are not shown. (c) The addition of unit cells with an electron in each one.

$$E_{10} = \frac{\pi^2\hbar^2}{2md^2}\left[\left(\frac{N_{el}}{2} + 1\right)^2 - \left(\frac{N_{el}}{2}\right)^2\right] = \frac{\pi^2\hbar^2}{2md^2}[N_{el} + 1]. \tag{15}$$

With the number of electrons given by

$$N_{el} = \frac{d}{a_0} \tag{16}$$

(one electron per cubic box of edge a_0), Eq. (15), with the help of Eq. (16), becomes

$$E_{10} = \frac{\pi^2\hbar^2}{2md^2}\left[\frac{d}{a_0} + 1\right] \underset{d\to\infty}{\Rightarrow} \frac{\pi^2\hbar^2}{2ma_0 d}. \tag{17}$$

Note that Eq. (17) scales as $1/d$. Later, we will see that for the three-dimensional box, where d is smaller than each of the two transverse directions, the energy difference scales as $1/\sqrt{d}$.

To determine the scaling of the limits of the polarizability, we substitute Eqs. (16) and (17) into Eq. (9), which yields

$$\alpha_{\max} = \frac{4a_0 me^2}{\pi^4\hbar^2}\cdot d^3 = \frac{4}{\pi^4}d^3, \tag{18}$$

where we have assumed that a_0 is the Bohr radius given by $a_0 = \hbar^2/me^2$. Since α is related to the volume of the molecule, it is not surprising that $\alpha_{\max}$ scales as d^3.

We can imagine that a material is made of a continuum where all molecules touch but otherwise do not interact. While this may seem like an unrealistic assumption, this case can be treated using local field models. The first-order susceptibility, the macroscopic quantity given simply by the ratio of the polarizability to the volume, is given by

$$\chi^{(1)}_{\max} = \frac{\alpha_{\max}}{da_0^2} = \frac{4}{\pi^4}\frac{d^2}{a_0^2}. \tag{19}$$

When far from resonances, the local field factors will change these values by perhaps a factor of two [12]—an amount that is of little consequence when describing order-of-magnitude numbers and large-exponent scaling.

The same procedure for a particle-in-a-box wave function can be applied to the hyperpolarizability and second hyperpolarizability. Using the fundamental limits

$$\beta_{\max} = \sqrt[4]{3}\left(\frac{e\hbar}{\sqrt{m}}\right)^3\cdot\frac{N_{el}^{3/2}}{E_{10}^{7/2}} \tag{20}$$

and

$$\gamma_{\max} = 4\left(\frac{e\hbar}{\sqrt{m}}\right)^4\cdot\frac{N_{el}^2}{E_{10}^5}, \tag{21}$$

and using the same approach as for α, it is straightforward to show that the hyperpolarizability and second hyperpolarizability in the long-length limit scale according to

$$\beta_{\max} = \frac{2^{7/2}3^{1/4}}{\pi^7}\cdot\frac{d^5}{e} \tag{22}$$

and

$$\gamma_{\max} = \frac{2^7}{\pi^{10}}\cdot\frac{d^7}{e^2}. \tag{23}$$

The second- and third-order susceptibilities are calculated by dividing Eqs. (22) and (23) by the volume of the box, yielding

$$\chi^{(2)}_{\max} = \left(\frac{3\cdot 2^{14}}{\pi^{28}}\right)^{1/4}\cdot\frac{d^4}{ea_0^2} \tag{24}$$

and

$$\chi^{(3)}_{\max} = \frac{2^7}{\pi^{10}}\cdot\frac{d^6}{e^2a_0^2}. \tag{25}$$

C. Spatial Dimensionality

In the previous section, we treated the classical and quantum cases in one dimension. In this section, we revisit the quantum case in three dimensions. We will consider only the induced dipole moment perpendicular to the large faces, the ramifications of which are discussed in Appendix A. This component can be isolated by experimental design with an electric field that is launched at the material with its polarization perpendicular to the slab. As such, electric dipole transitions will be induced without affecting the transverse parts of the wavefunction.

If the slab is made of a conductor, we can subdivide it into cubes that each contribute one conduction electron. As the slab is made larger by adding cubes, the number of electrons increases in proportion to the volume but each energy eigenvalue decreases. The energy, $e_{n,p,q}$, of the nth quantum number corresponding to the part of the wave function along the surface normal and the pth and qth transverse quantum numbers of a single particle in a box is given by

$$e_{n,p,q} = \frac{\pi^2\hbar^2}{2m}\left(\frac{n^2}{d^2}+\frac{p^2}{L_1^2}+\frac{q^2}{L_2^2}\right), \tag{26}$$

where L_1 and L_2 are the two transverse dimensions of the box.

Assuming that the electrons do not interact with each other, the single-particle states will be filled according to the Pauli exclusion principle while taking into account the quantum numbers of the transverse parts of the wave function. Since the lateral dimensions are larger than the thickness of the slab, the energy spacing of the transverse states will be more closely packed than the perpendicular component. As such, for a given quantum number n in Eq. (26), there will be many transverse quantum numbers that make distinct states that need to be filled before the next-higher energy eigenstate indexed by $n+1$ gets filled.

For an experiment that only excites the perpendicular component, given by a change in only n, there will be many states corresponding to pairs of p and q quantum numbers that remain unchanged. As such, these states will not contribute to the optical response and so can be ignored. However, the determination of how many states are occupied still requires the transverse states to be counted when determining the value of n associated with the Fermi level. The net effect is that few electrons participate in the excitations that contribute to the nonlinear response. Appendix A describes the approach for taking into account these quantum numbers.

Figure 2(a) shows a box of width $2a_0$, which holds two electrons. When the box size is made bigger by adding more material, for every additional length $2a_0$, two more electrons will be added. In addition, the larger box will yield more closely spaced energy levels. Figure 2(b) shows a box that is three times wider than the one shown in Fig. 2(a). As such, its energy levels are compressed accordingly.

In the two-electron box, the first excited state energy is calculated by promoting one electron to the next higher state. This yields $E_{10} = e_2 - e_1$ (e_i represents the single-electron energy and E_i the many-electron state energy). The six-electron box yields $E_{10} = e_4 - e_3$. As such, the general case for a Fermi level at state n yields

$$E_{10} = e_{n+1} - e_n. \tag{27}$$

Using the single-particle energy levels given by Eq. (26) with q and p unchanged, E_{10} in the asymptotic limit—as described in Appendix A by Eq. (A5)—is then given by

$$\begin{aligned} E_{10} &= \frac{\pi^2\hbar^2}{2md^2}\left[\left(\sqrt{\frac{2d^2N_{el}}{\pi L_1L_2}}+1\right)^2-\frac{2d^2N_{el}}{\pi L_1L_2}\right] \\ &= \frac{\pi^2\hbar^2}{2md^2}\left(\sqrt{\frac{8d^2N_{el}}{\pi L_1L_2}}+1\right). \end{aligned} \tag{28}$$

Recall that the fundamental limit of the polarizability is given by

$$\alpha_{\max} = \frac{e^2\hbar^2}{m}\cdot\frac{N_{el}}{E_{10}^2}, \tag{29}$$

where N_{el} is the number of electrons, E_{10} the energy difference between the ground and first excited state, and the others are the usual constants. The energy difference can be calculated using Eq. (27), and the number of electrons is given by

$$N_{el} = \frac{L_1L_2d}{a_0^3} = \frac{L_1}{a_0}\cdot\frac{L_2}{a_0}\cdot\frac{d}{a_0}, \tag{30}$$

where we use the fact that there is one electron per volume a_0^3. Thus, for large N_{el}, Eq. (28) with the help of Eq. (30) yields

$$E_{10} = \frac{\pi\hbar^2}{ma_0}\sqrt{\frac{2\pi}{a_0d}} = \sqrt{2}\pi^{3/2}\cdot\frac{\hbar^2}{ma_0^2}\cdot\sqrt{\frac{a_0}{d}}. \tag{31}$$

The last equality expresses the result in terms of the ratio of a_0 and d and constants that are grouped together to give units of energy.

The scaling of the polarizability for the 3D box is determined by substituting Eqs. (30) and (31) into Eq. (29), yielding

$$\alpha_{\max} = \frac{me^2}{2\pi^3\hbar^2}\cdot Ad^2 = \frac{1}{2\pi^3}\cdot Ad\frac{d}{a_0}, \tag{32}$$

where we have used $A = L_1L_2$ and where a_0 is the Bohr radius given by $a_0 = \hbar^2/me^2$. The linear susceptibility is then given by the polarizability divided by the volume, or

$$\chi^{(1)}_{\max} = \frac{1}{2\pi^3}\cdot\frac{d}{a_0}. \tag{33}$$

Table 1 summarizes the polarizabilities and first-order susceptibilities of the quantum box in 1D and 3D and the classical box.

The nonlinear susceptibility limits are calculated in the same way, yielding

$$\beta_{\max} = \left(\frac{3}{2\cdot\pi^{21}}\right)^{1/4}\cdot\frac{A^{3/2}a_0^2}{e}\cdot\left(\frac{d}{a_0}\right)^{13/4} \tag{34}$$

and

Table 1. Columns Represent α_{max}, the Volume of the Object, and an Expression for $\chi^{(1)}$[a]

	α_{max}	Volume	$\chi^{(1)} = \alpha_{max}/\text{volume}$	$\chi^{(1)}(d = 100a_0, \varepsilon = 2.25)$
Quantum 1D	$\frac{4}{\pi^4}\cdot\frac{a_b}{a_0}\cdot d^3 \underset{a_0\approx a_b}{\Longrightarrow} \frac{4}{\pi^4}\cdot d^3$	da_0^2	$\frac{4}{\pi^4}\cdot\frac{d^2}{a_0^2}$	4×10^3
Quantum 3D	$\frac{1}{2\pi^3}\cdot\frac{A}{a_0}\cdot d^2$	Ad	$\frac{1}{2\pi^2}\cdot\frac{d}{a_0}$	5
Classical 3D	$Ad\left(\frac{\varepsilon(\omega)-1}{4\pi\varepsilon(\omega)}\right)$	Ad	$\frac{\varepsilon(\omega)-1}{4\pi\varepsilon(\omega)}$	0.04

[a]The last column represents $\chi^{(1)}$ for an object of length $100a_0$ and for a relative permittivity of $\varepsilon = 2.25$, as is common for transparent materials in the visible part of the spectrum.

$$\gamma_{max} = \frac{1}{\sqrt{2\cdot\pi^{15}}}\cdot\frac{A^2a_0^3}{e^2}\cdot\left(\frac{d}{a_0}\right)^{9/2}. \quad (35)$$

Dividing the hyperpolarizabilities by the volume $A\cdot d$ yields the bulk susceptibilities

$$\chi^{(2)}_{max} = \left(\frac{3}{2\cdot\pi^{21}}\right)^{1/4}\cdot\frac{A^{1/2}a_0}{e}\cdot\left(\frac{d}{a_0}\right)^{9/4} \quad (36)$$

and

$$\chi^{(3)}_{max} = \frac{1}{\sqrt{2\cdot\pi^{15}}}\cdot\frac{Aa_0^2}{e^2}\cdot\left(\frac{d}{a_0}\right)^{7/2}. \quad (37)$$

3. RESULTS AND DISCUSSION

Table 1 summarizes the scaling of the polarizabilities and first-order susceptibilities for quantum 1D and 3D limits and classical 3D plasmonic systems. The quantum 1D and 3D polarizabilities scale as the length of the system to the third and second powers, while the classical system scales linearly with length. More telling is the linear susceptibility, which is independent of size in the classical system and scales as d^2 and d in the quantum 1D and 3D cases. The last column shows the linear susceptibilities for a transparent material with a refractive index of $n = 1.5$. The quantum 1D system is clearly the best.

Table 2 summarizes the scaling of 1D and 3D quantum systems. Again, the 1D case beats the 3D case in all orders of nonlinearity and the higher orders scale more favorably with length than the lower-order ones.

It is worthwhile to evaluate the scaling expressions calculated here to get a sense of the magnitude of the nonlinear response that may be attainable. Assuming that one can make a structure that retains quantum coherence over a length of $d = 100$ Å ($d = 100a_0$), this one-dimensional nanoscale system—according to Eq. (22)—will have $\beta = 10^{-23}$ cm$^5\cdot$statvolt^{-1}. In comparison, the largest second-order susceptibility ever calculated is $\beta = 2.6\times10^{-26}$ cm$^5\cdot$statvolt^{-1} for a huge molecule made with coupled porphyrins that has approximately the same number of electrons as the nanorod calculated here [13].

A 3D system with the same number of electrons will necessarily be much shorter since the transverse dimension must be larger than the length. Assuming $A = 100a_0^2$, then $d = a_0$ and Eq. (34) gives $\beta = 6\times10^{-31}$ cm$^5\cdot$statvolt^{-1}. The one-dimensional system thus uses electrons much more effectively, yielding a hyperpolarizability that is almost eight orders of magnitude larger than the 3D case.

The second-order susceptibility of the 100 Å linear system is $\chi^{(2)} = 0.1$cm$^2\cdot$statvolt^{-1} and the 3D case yields $\chi^{(2)} = 6\times10^{-9}$ cm$^2\cdot$statvolt^{-1}. In more familiar units, these are $\chi^{(2)} = 3\times10^6$ pm/V and $\chi^{(2)} = 6\times10^{-2}$ pm/V, respectively. The very best materials are at $\chi^{(2)} = 500$ pm/V [14]. Thus, the best materials demonstrated to date fall far below what is possible in a 1D system but exceed the maximum values allowed in 3D systems.

The second hyperpolarizability and third-order susceptibilities can be evaluated in the same way. Using Eqs. (23) and (35), these yield $\gamma = 6\times10^{-27}$ cm$^7\cdot$statcoul^{-2} and $\gamma = 6\times10^{-38}$ cm$^7\cdot$statcoul^{-2}, respectively. The best molecules have $\gamma = 5\times10^{-32}$ cm$^7\cdot$statcoul^{-2} [15]. As was the case for the hyperpolarizability, the best molecule measured is larger than the 3D limit but far short of the 1D limit—in this case, by five orders of magnitude.

While the 100 Å systems have ultralarge nonlinear-optical response, perhaps they can be made even larger. Consider, for example, $\chi^{(3)}$ of a 1D system. The third-order susceptibility scales as d^6. If a molecule is made twice as long, $\chi^{(3)}$ becomes almost two orders of magnitude larger. If the molecule can be increased in length by a factor of 10, $\chi^{(3)}$ is enhanced a million-fold. The bottleneck to extending the length is in the coherence of the wave function. The values calculated above are in the gray region where quantum coherence is lost, leading to classical behavior. Gaining a better understanding of what determines the critical length could be used to extend it. Even modest increases in the critical length could lead to much larger nonlinear response.

Table 2. Scaling of the Fundamental Limits of Various Orders of Nonlinearity as a Function of Length for a 1D and 3D Box

	Fundamental Limits	1D Box Scaling	3D Box Scaling
α_{max}	$\frac{e^2\hbar^2}{m}\cdot\frac{N_{el}}{E_{10}^2}$	$\frac{4}{\pi^4}d^3$	$\frac{1}{2\pi^3}\cdot Ad\frac{d}{a_0}$
β_{max}	$\sqrt[4]{3}\left(\frac{e\hbar}{\sqrt{m}}\right)^3\cdot\frac{N_{el}^{3/2}}{E_{10}^{7/2}}$	$\frac{2^{7/2}3^{1/4}}{\pi^7}\cdot\frac{d^5}{e}$	$\left(\frac{3}{2\cdot\pi^{21}}\right)^{1/4}\cdot\frac{A^{3/2}a_0^2}{e}\cdot\left(\frac{d}{a_0}\right)^{13/4}$
γ^{max}	$4\left(\frac{e\hbar}{\sqrt{m}}\right)^4\cdot\frac{N_{el}^2}{E_{10}^5}$	$\frac{2^7}{\pi^{10}}\cdot\frac{d^7}{e^2}$	$\frac{1}{\sqrt{2\cdot\pi^{15}}}\cdot\frac{A^2a_0^3}{e^2}\cdot\left(\frac{d}{a_0}\right)^{9/2}$

4. CHEATING NATURE

All molecules measured and all quantum systems calculated fall short of the fundamental limits. Perhaps there are clever ways to construct a quantum system that might break the limits. For example, decades ago, Birnboim and coworkers proposed that local field enhancements could beef up the nonlinear response by several orders of magnitude [16,17] and reported on optical bistability experiments that showed enhancements in metals coated with nonlinear-optical molecules [18].

In principle, the local field enhancement due to a surface plasmon excited in a metal particle at the appropriate frequency

can enhance the electric field at the surface by two orders of magnitude above the incident field strength. Since the radiation induced through the second hyperpolarizability is proportional to the fourth power of the electric field, the net enhancement of a third-order process can be as high as 10^8. The nonlinear response of a molecule whose nonlinear-optical response is a couple orders of magnitude below the limit will be significantly higher than the limit when placed in the region of an intensified electric field near a metal particle.

While the effective nonlinear-optical response can indeed beat the limits in this way, the fallacy is in not including all the electrons of the combined system. Since the surface plasmon resonance is a classical phenomenon, many electrons contribute and the nonlinear response of the combined system is well below the limit because the vast majority of the electrons are not used effectively. Furthermore, the enhanced electric field is found only at localized hot spots near the nanoparticle. Consequently, the bulk material's nonlinear response will be low due to the low density of hot spots. Thus, it is far better to make many quantum objects than a single quantum object placed near a large particle that wastes electrons.

Another approach to breaking the limits is to use exotic Hamiltonians. Atherton reported that Hamiltonians that are not Hermitian but invariant under the combined action of time reversal and parity [19] can break the limits [20]. There are no known systems that behave according to such Hamiltonians. However, a composite system made of many particles, such as Bose–Einstein condensates, might behave in this way. While a quasi-particle that is governed by an exotic Hamiltonian might appear to break the limits, the system as a whole is well within the upper bounds when all of the charges that make the quasi-particle are counted. The important point here is that the full system is still Hermitian, but a subsystem may act as if it were non-Hermitian. If all electrons were counted, the limits would not be broken. However, investigations of such systems might lead to new insights that are applicable to finding new ways to make materials with a larger intrinsic nonlinear response.

An example of how nature can be fooled to yield a large intensity-dependent refractive index was shown by Boyd's group in indium tin oxide (ITO), which has a dielectric constant near zero [21]. To understand the underlying principles, consider the dielectric constant, ε, which through a third-order process depends on the intensity according to $\varepsilon = \varepsilon_0 + \varepsilon_2 E^2$, yielding the intensity-dependent refractive index

$$n = \sqrt{\varepsilon} = \sqrt{\varepsilon_0}\left(1 + \frac{\varepsilon_2 E^2}{\varepsilon_0}\right)^{1/2} \equiv n_0\left(1 + \frac{\varepsilon_2 E^2}{n_0^2}\right)^{1/2}, \quad \textbf{(38)}$$

where n_0 is the zero-intensity refractive index. Since the change in the refractive index for typical intensities is small compared with n_0, Eq. (38) can be well approximated by a power series to order $\varepsilon_2 E^2$, yielding

$$n \approx n_0 + \frac{\varepsilon_2 E^2}{2n_0}, \quad \textbf{(39)}$$

which holds only when $\frac{\varepsilon_2 E^2}{2n_0} \ll n_0$.

If one forgets that Eq. (39) is a series approximation, it would seem to imply that an infinite refractive index change is possible when $n_0 \to 0$. To get the correct refractive index change in the limiting case $n_0 \to 0$ requires that the exact expression given by Eq. (38) be evaluated. In the limit where the refractive index vanishes so that $\frac{\varepsilon_2 E^2}{n_0^2} \gg 1$, Eq. (38) can be approximated by

$$n \approx \sqrt{\varepsilon_2} E. \quad \textbf{(40)}$$

Thus, in the low $\varepsilon_2 E^2/n_0$ approximation, the change in the refractive index is proportional to the square of the electric field E^2 while for large $\varepsilon_2 E^2/n_0$, the refractive index change is proportional to the electric field.

To put this into perspective by numerical example, when the refractive index change $\Delta n = \varepsilon_2 E^2$ is small—let us say of the order of $\Delta n = 10^{-4}$, as is typical—and then when the refractive index vanishes, the refractive index change is $\Delta n = 10^{-2}$. As such, smaller refractive index changes give larger enhancements.

The enhancement can be made to look even greater when the refractive index change is expressed in terms of the intensity or in the form $n = n_0 + n_2 I$. Then, $n_2 \propto \varepsilon_2/n_0$. When n_0 vanishes, the intensity-dependent refractive index can diverge. However, when the real part of the relative permittivity vanishes in ITO, $\varepsilon = 0.4i$, so the magnitude of the refractive index does not vanish.

The key point here is that the fundamental nonlinearity γ is indeed bounded, which places a limit on the induced dipole moment for a given electric field, which is also bounded. The refractive index and the intensity are not fundamental quantities but observables that derive from the fundamental quantities. It is thus possible for ratios of quantities to give infinite results when the denominator vanishes.

This is an important point that is missed in the quest for making materials with a large nonlinear-optical susceptibility. The nonlinear susceptibility alone may not be the quantity of interest. Rather, composite properties such as the FOM for an application may be a more appropriate parameter for optimization. In fact, a FOM may be large when the nonlinearity is small. Thus, material designs would be more effective when the FOM is the quantity targeted. This ground-up approach for electro-optic modulators shows that low optical loss may be more important than high nonlinearity [22].

The limits of the hyperpolarizabilities are observed to be obeyed for all classical and quantum systems. As such, we focus on these upper bounds with the understanding that specific applications have requirements that are quantified by figures of merit that may not have an upper bound. However, since the figures of merit depend on fundamental properties—each governed by quantum principles—these properties cannot be individually adjusted.

5. CONCLUSION AND PERSPECTIVES

The intrinsic nonlinear-optical response is used as a metric to identify those underlying properties of a material that are critical to optimizing the bulk nonlinear-optical response. The process starts at the microscopic level to identify which molecular paradigms give the largest nonlinearity for a given size, as characterized by the intrinsic nonlinearity. Then, the dependence of the nonlinearity is studied as a function of the system size. A quantum system with a large intrinsic nonlinear-optical response that it retains when it is made larger will have a huge

absolute nonlinear susceptibility. The scaling of a particle in a box model was used for illustration and found to scale as a power law when unit cells are added to both increase length and add electrons. On 100 Å scales, the predicted nonlinearities are orders of magnitude larger than the best systems reported.

The power-law length dependence implies that nonlinearities can be made much larger when the system is made marginally longer, provided that the nonlinear response is of quantum mechanical origin. It is found that the ideal quantum unit is one-dimensional because transverse states dilute the strength of the nonlinearity by rendering a majority of the electrons ineffective. A system that is larger than the critical size, where a classical response dominates, no longer takes advantage of increased size. At this point, it would be worthwhile to investigate methods for retaining quantum behavior on larger length scales.

Finally, the quantum units need to be arranged in a way that gives the largest nonlinear response. The one-dimensional units should be parallel to each other so that the nonlinearly of each unit is reinforced and the density should be as high as possible. A large second-order susceptibility requires a polar-aligned material and a large third-order susceptibility requires an axially aligned material. Figure 3 shows the ideal material.

Since the size of the ideal molecular units borders on the classical realm and requires high electron density, it will most likely be a metal, rigid metallic polymer or a hybrid system made of interacting nanoscale particles and molecules. Second, the wave functions will need to be precisely controlled to optimize the overlap between the ground state and the two dominant excited states. Possible avenues include using impurities [23], modulated conjugation of molecular bonds [24], or topology that controls the placement of kinks in the wave functions [25]. The units that make up the material could be aligned with the application of an electric or magnetic field, local steric forces such as those in liquid crystals, or using chemical bonds as spacers that hold the individual units together [26–28].

The requirement of one-dimensional units originates in the dipole approximation, which governs the strength of the induced electric dipole moment by an electric field. While electric dipole excitations generally give larger susceptibilities than the magnetic dipole term, there may be ways to get a larger response in a magnetic material. A magnetic dipole is a current running in a closed loop, so it is inherently a planar structure. Since the nonlinear response in this case should grow as a power law of the area, and the area grows in proportion to the square of the diameter, it may be possible to find systems that are just as good, if not better than electric dipolar ones, if they can be made large enough.

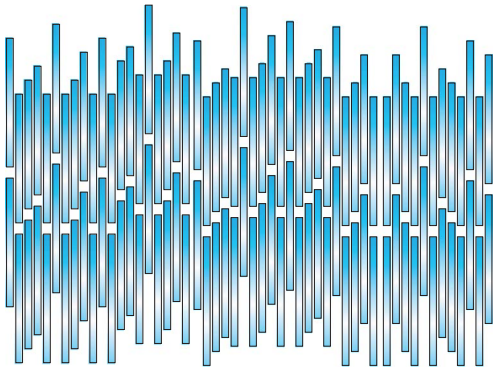

Fig. 3. Ideal second-order nonlinear-optical material is made of one-dimensional polar objects that are each as large as possible without showing quantum behavior and packed to maximum density. A third-order susceptibility requires axial order.

The central result in this work is that the nonlinear response of molecular units is optimized if the system is described by quantum excitations of a 1D structure. At the other extreme, where a system is large enough to behave classically, the local fields are enhanced as one finds in plasmonic systems, an effect known for decades [29–31], and years ago was applied to enhancing the second-harmonic efficiency [32]. However, as we have shown, a system of classical size uses its electrons ineffectively, ironically making plasmonic systems the least efficient users of electrons. It is proposed here that the ideal balance starts with the design of molecular units using quantum principles and making them as long as possible until the point of diminishing returns is reached. Then, aggregates of the molecular units can be made to interact with each other in ways that intensify the molecular response. This use of hierarchies allows a material to best take advantage of its electrons on all length scales. While no such system can beat the fundamental limits when all the electrons are counted, a hierarchical design might lead to huge absolute nonlinear response that exceeds the best materials by many orders of magnitude.

When a material is being designed for a particular application, the FOM needs to be optimized. Since figures of merit are often not fundamental quantum properties, they can be arbitrarily large. In these cases, one can model the FOM in terms of fundamental parameters (such as hyperpolarizability and loss) to find the ultimate material design.

The approaches outlined here are difficult to implement and rely on fundamental properties that are not intuitively obvious to a synthetic chemist or a material scientist. In contrast, traditional approaches used to design better materials are more intuitive but lead to only incremental improvements. This paper shows that using the fundamental limits and intrinsic nonlinearities as a guide to designing better materials offers the promise of many-orders-of-magnitude improvements in the nonlinear response or FOMs.

APPENDIX A: FILLING THE STATES OF A BOX

In a rectangular box, each energy eigenfunction is expressed as the product of three wave functions along the three Cartesian axes that are perpendicular to the walls of the box. First, we determine which pairs of transverse quantum numbers p and q contribute an energy less than that due to the quantum number n associated with the longitudinal contribution. We define the longitudinal direction to be along the applied electric field.

Figure 4(a) shows the energy-level diagram of the three Cartesian components. The task at hand is to determine the quantum number n for highest-energy occupied state given that N_{el} electrons fill the box. To do so requires a calculation of the number of transverse states with energy less than the energy of state n.

According to Eq. (26), the transverse contribution due to the pair of quantum numbers p and q is less than due to the longitudinal state n when

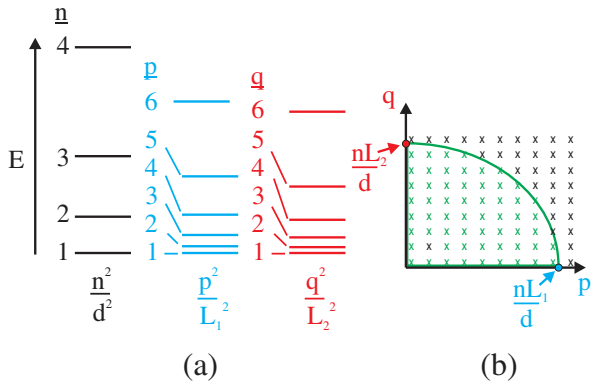

Fig. 4. (a) n, p, and q quantum numbers used in determining the energy, and (b) the curve that represents all the p and q quantum numbers that contribute an energy less than that of the contribution due to quantum number n.

$$\frac{n^2}{d^2} < \frac{p^2}{L_1^2} + \frac{q^2}{L_2^2}, \tag{A1}$$

where L_1 and L_2 are the lengths of the two transverse edges of the box. Figure 4(b) shows a plot of this boundary and the green crosses show all pairs of p and q with energy less than that due to the longitudinal contribution.

Equation (A1) defines an ellipse whose area in the first quadrant (due to the restriction that all quantum numbers are positive) determines the number of pairs of quantum numbers that we seek. The number of states is thus given by

$$g(n) = \pi \frac{L_1 L_2}{4d^2} n^2. \tag{A2}$$

The total number of electrons for a system filled to quantum number n is then given by

$$N_{el} = 2n + 2g(n) = 2n + \pi \frac{L_1 L_2}{2d^2} n^2, \tag{A3}$$

where we fill each state with two electrons.

Solving Eq. (A3) for n yields the highest occupied state,

$$n = \frac{-1 \pm \sqrt{1 + \pi \frac{L_1 L_2}{2d^2} N_{el}}}{\pi \frac{L_1 L_2}{2d^2}}. \tag{A4}$$

Omitting the unphysical negative solution for n, the asymptotic solution to Eq. (A4) when the transverse dimensions L_1 and L_2 are much larger than d gives

$$n \to \sqrt{\frac{2}{\pi} \cdot \frac{d^2}{L_1 L_2} \cdot N_{el}}. \tag{A5}$$

Note that in the limiting case where $d^2 \gg L_1 L_2$, Eq. (A4) gives $n = N_{el}/2$, which is in agreement with what we expect for the one-dimensional case.

Funding. Directorate for Engineering (ENG) (ECCS-1128076).

Acknowledgment. I acknowledge the Meyer Distinguished Professorship of the Sciences for generously supporting this work.

REFERENCES

1. R. Roberts, T. Schwich, T. Corkery, M. Cifuentes, K. Green, J. Farmer, P. Low, T. Marder, M. Samoc, and M. Humphrey, "Organometallic complexes for nonlinear optics. 45. dispersion of the third-order nonlinear optical properties of triphenylamine-cored alkynylruthenium dendrimers," Adv. Mater. **21**, 2318–2322 (2009).
2. A. D. Slepkov, F. A. Hegmann, S. Eisler, E. Elliot, and R. R. Tykwinski, "The surprising nonlinear optical properties of conjugated polyyne oligomers," J. Chem. Phys. **120**, 6807–6810 (2004).
3. S. Eisler, A. Slepkov, E. Elliott, T. Luu, R. McDonald, F. Hegmann, and R. Tykwinski, "Polyynes as a model for carbyne: synthesis, physical properties, and nonlinear optical response," J. Am. Chem. Soc. **127**, 2666–2676 (2005).
4. T. Luu, E. Elliott, A. Slepkov, S. Eisler, R. McDonald, F. Hegmann, and R. Tykwinski, "Synthesis, structure, and nonlinear optical properties of diarylpolyynes," Org. Lett. **7**, 51–54 (2005).
5. J. Pérez Moreno and K. Clays, "Fundamental limits: developing new tools for a better understanding of second-order molecular nonlinear optics," J. Nonlinear Opt. Phys. Mater. **18**, 401–440 (2009).
6. J. A. Scholl, A. L. Koh, and J. A. Dionne, "Quantum plasmon resonances of individual metallic nanoparticles," Nature **483**, 421–427 (2012).
7. H. Kuhn, "Free electron model for absorption spectra of organic dyes," J. Chem. Phys. **16**, 840–841 (1948).
8. H. Kuhn, "A quantum-mechanical theory of light absorption of organic dyes and similar compounds," J. Chem. Phys. **17**, 1198–1212 (1949).
9. W. Kuhn, "Über die Gesamtstarke der von einem Zustande ausgehenden Absorptionslinien," Z. Phys. A **33**, 408–412 (1925).
10. F. Reiche and U. W. Thomas, "Über die Zahl der Dispersionselektronen, die einem stationären Zustand zugeordnet sind," Z. Phys. **34**, 510–525 (1925).
11. W. Thomas, "Über die Zahl der Dispersionselektronen, die einem stationären Zustande zugeordnet sind (Vorlaufige Mitteilung)," Naturwissenschaften **13**, 627 (1925).
12. J. J. Maki, M. S. Malcuit, J. E. Sipe, and R. W. Boyd, "Linear and nonlinear optical measurements of the Lorentz local field," Phys. Rev. Lett. **67**, 972–975 (1991).
13. N. Jiang, G. Zuber, S. Keinan, A. Nayak, W. Yang, M. Therien, and D. Beratan, "Design of coupled porphyrin chromophores with unusually large hyperpolarizabilities," J. Phys. Chem. C **116**, 9724–9733 (2012).
14. L. Dalton, P. Sullivan, and D. Bale, "Electric field poled organic electro-optic materials: state of the art and future prospects," Chem. Rev. **110**, 25–55 (2010).
15. J. Perez-Moreno, S. Shafei, and M. G. Kuzyk, "Applying universal scaling laws to identify the best molecular design paradigms for third-order nonlinear optics," arXiv:1604.03779 (2016).
16. A. E. Neeves and M. H. Birnboim, "Composite structures for the enhancement of nonlinear optical materials," Opt. Lett. **13**, 1087–1089 (1988).
17. A. E. Neeves and M. H. Birnboim, "Composite structures for the enhancement of nonlinear-optical susceptibility," J. Opt. Soc. Am. B **6**, 787–796 (1989).
18. N. Kalyaniwalli, J. W. Haus, R. Inguva, and M. H. Birnboim, "Intrinsic optical bistability for coated spheroidal particles," Phys. Rev. A **42**, 5613–5621 (1990).
19. C. M. Bender, "Making sense of non-Hermitian Hamiltonians," Rep. Prog. Phys. **70**, 947–1018 (2007).
20. T. Atherton, "Hyperpolarizabilities of exotic potentials," in *Foundations of Nonlinear Optics* (Lehigh University, 2016).
21. M. Zahirul Alam, I. De Leon, and R. W. Boyd, "Large optical nonlinearity of indium tin oxide in its epsilon-near-zero region," Science **352**, 795–797 (2016).
22. S. Mossman, R. Lytel, and M. G. Kuzyk, "Fundamental limits on the electro-optic device figure of merit," arXiv:1607.06052 (2016).
23. B. Coe, J. Harris, B. Brunschwig, I. Asselberghs, K. Clays, J. Garn, and J. Orduna, "Three-dimensional nonlinear optical chromophores based on metal-to-ligand charge-transfer from ruthenium (ii) or iron (ii) centers," J. Am. Chem. Soc. **127**, 13399–13410 (2005).
24. J. Pérez-Moreno, Y. Zhao, K. Clays, and M. G. Kuzyk, "Modulated conjugation as a means for attaining a record high intrinsic hyperpolarizability," Opt. Lett. **32**, 59–61 (2007).

25. R. Lytel, S. Mossman, and M. Kuzyk, "Phase disruption as a new design paradigm for optimizing the nonlinear-optical response," Opt. Lett. **40**, 4735–4738 (2015).
26. A. W. Harper, S. Sun, L. R. Dalton, S. M. Garner, A. Chen, S. Kalluri, W. H. Steier, and B. H. Robinson, "Translating microscopic optical nonlinearity into macroscopic optical nonlinearity: the role of chromophore–chromophore electrostatic interactions," J. Opt. Soc. Am. B. **15**, 329–337 (1998).
27. B. Robinson, L. Dalton, A. Harper, A. Ren, F. Wang, C. Zhang, G. Todorova, M. Lee, R. Aniszfeld, and S. Garner, "The molecular and supramolecular engineering of polymeric electro-optic materials," Chem. Phys. **245**, 35–50 (1999).
28. L. Dalton, S. Benight, L. Johnson, D. Knorr, Jr., I. Kosilkin, B. Eichinger, B. Robinson, A. Jen, and R. Overney, "Systematic nanoengineering of soft matter organic electro-optic materials," Chem. Mater. **23**, 430–445 (2011).
29. A. A. Lushnikov, V. V. Maksimenko, and A. J. Simonov, "Surface plasmons in small layer metal particles," Solid State Commun. **20**, 545–547 (1976).
30. G. C. Papavassiliou, "Surface plasmons in small Au–Ag alloy particles," J. Phys. F **6**, L103–L105 (1976).
31. H. J. Simon, R. E. Benner, and J. G. Rako, "Optical second harmonic generation with surface plasmons in piezoelectric crystals," Opt. Lett. **23**, 245–248 (1977).
32. C. K. Chen, A. R. B. D. Castro, and Y. R. Shen, "Coherent second-harmonic generation by counterpropagating surface plasmons," Opt. Lett. **4**, 393–394 (1979).